3. I. F. Sevrioukova, C. Garcia, H. Li, B. Bhaskar, T. L. Poulos, *J. Mol. Biol.* **333**, 377 (2003).
4. I. F. Sevrioukova, H. Li, T. L. Poulos, *J. Mol. Biol.* **336**, 889 (2004).
5. I. F. Sevrioukova, T. L. Poulos, I. Y. Churbanova, *J. Biol. Chem.* **285**, 13616 (2010).
6. I. C. Gunsalus, J. R. Meeks, J. D. Lipscomb, *Ann. N. Y. Acad. Sci.* **212**, (1 Multienzyme S), 107 (1973).
7. J. D. Lipscomb, S. G. Sligar, M. J. Namtvedt, I. C. Gunsalus, *J. Biol. Chem.* **251**, 1116 (1976).
8. S. G. Sligar, P. G. Debrunner, J. D. Lipscomb, M. J. Namtvedt, I. C. Gunsalus, *Proc. Natl. Acad. Sci. U.S.A.* **71**, 3906 (1974).
9. C. A. Tyson, J. D. Lipscomb, I. C. Gunsalus, *J. Biol. Chem.* **247**, 5777 (1972).
10. T. C. Pochapsky, T. A. Lyons, S. Kazanis, T. Arakaki, G. Ratnaswamy, *Biochimie* **78**, 723 (1996).
11. S. Nagano *et al.*, *Biochemistry* **42**, 14507 (2003).
12. S. S. Pochapsky, T. C. Pochapsky, J. W. Wei, *Biochemistry* **42**, 5649 (2003).
13. Y. Shiro, T. Iizuka, R. Makino, Y. Ishimura, I. Morishima, *J. Am. Chem. Soc.* **111**, 7707 (1989).
14. T. Tosha *et al.*, *J. Biol. Chem.* **278**, 39809 (2003).
15. M. Unno *et al.*, *J. Biol. Chem.* **277**, 2547 (2002).
16. W. Zhang, S. S. Pochapsky, T. C. Pochapsky, N. U. Jain, *J. Mol. Biol.* **384**, 349 (2008).
17. Y. T. Lee, R. F. Wilson, I. Rupniewski, D. B. Goodin, *Biochemistry* **49**, 3412 (2010).
18. I. F. Sevrioukova, H. Li, H. Zhang, J. A. Peterson, T. L. Poulos, *Proc. Natl. Acad. Sci. U.S.A.* **96**, 1863 (1999).
19. N. Strushkevich *et al.*, *Proc. Natl. Acad. Sci. U.S.A.* **108**, 10139 (2011).
20. M. Guo, B. Bhaskar, H. Li, T. P. Barrows, T. L. Poulos, *Proc. Natl. Acad. Sci. U.S.A.* **101**, 5940 (2004).
21. M. Unno *et al.*, *J. Am. Chem. Soc.* **119**, 6614 (1997).
22. H. Koga *et al.*, *FEBS Lett.* **331**, 109 (1993).
23. K. Nakamura *et al.*, *Biochim. Biophys. Acta* **1207**, 40 (1994).
24. H. Shimada, S. Nagano, H. Hori, Y. Ishimura, *J. Inorg. Biochem.* **83**, 255 (2001).
25. V. Y. Kuznetsov *et al.*, *J. Biol. Chem.* **280**, 16135 (2005).
26. S. Nagano, T. L. Poulos, *J. Biol. Chem.* **280**, 31659 (2005).
27. I. Schlichting *et al.*, *Science* **287**, 1615 (2000).
28. N. C. Gerber, S. G. Sligar, *J. Biol. Chem.* **269**, 4260 (1994).

Acknowledgments: This work was supported by NIH grant GM33688. Portions of this research were carried out at the Stanford Synchrotron Radiation Lightsource (SSRL), a Directorate of SLAC National Accelerator Laboratory and an Office of Science User Facility operated for the U.S. Department of Energy (DOE) Office of Science by Stanford University. The SSRL Structural Molecular Biology Program is supported by the DOE Office of Biological and Environmental Research and by NIH, the National Institute of General Medical Sciences (NIGMS) (including P41GM103393), and the National Center for Research Resources (NCRR) (P41RR001209). The contents of this publication are solely the responsibility of the authors and do not necessarily represent the official views of NIGMS, NCRR, or NIH. We also acknowledge the Advanced Light Source supported by the Director, Office of Science, Office of Basic Energy Sciences, of the DOE under contract DE-AC02-05CH11231. We thank C. Goulding and A. Borovik for invaluable discussions and advice, D. Goodin for the low Cys P450cam expression plasmid, and Y. Meharenna for assistance in developing cross-linking protocols.

Supplementary Materials

www.sciencemag.org/cgi/content/full/340/6137/1227/DC1
Materials and Methods
Figs. S1 to S6
Tables S1 and S2
References (*29*–*42*)

29 January 2013; accepted 10 April 2013
10.1126/science.1235797

Role of Tissue Protection in Lethal Respiratory Viral-Bacterial Coinfection

Amanda M. Jamieson,[1,2]*†‡ Lesley Pasman,[1]‡ Shuang Yu,[1] Pia Gamradt,[2] Robert J. Homer,[3,4] Thomas Decker,[2] Ruslan Medzhitov[1]*

Secondary bacterial pneumonia leads to increased morbidity and mortality from influenza virus infections. What causes this increased susceptibility, however, is not well defined. Host defense from infection relies not only on immune resistance mechanisms but also on the ability to tolerate a given level of pathogen burden. Failure of either resistance or tolerance can contribute to disease severity, making it hard to distinguish their relative contribution. We employ a coinfection mouse model of influenza virus and *Legionella pneumophila* in which we can separate resistance and tolerance. We demonstrate that influenza virus can promote susceptibility to lethal bacterial coinfection, even when bacterial infection is controlled by the immune system. We propose that this failure of host defense is due to impaired ability to tolerate tissue damage.

Resistance and tolerance are two distinct strategies of host defense from infections: the former is based on pathogen detection and elimination, whereas the latter relies on host adaptation to a given level of pathogen burden (*1*–*4*). This distinction is important because infectious disease morbidity and mortality can be due to failed resistance or failed tolerance, which may, in turn, dictate different therapeutic options. Thus, a lethal outcome of microbial infection is usually ascribed to either high pathogen virulence or low host resistance (for example, caused by immunosuppression or immunodeficiency). Pathogen virulence can be due to direct damage to the host by toxins and virulence factors (intrinsic virulence) or, more commonly, due to excessive inflammatory response with collateral tissue damage (extrinsic virulence). However, insufficient tissue protection and repair could also be an important contributor to infectious disease phenotypes (*4*).

The upper respiratory tract is exposed to numerous pathogens simultaneously, and viral-bacterial coinfection in the lung is a common clinical manifestation [reviewed in (*5*–*8*)]. Complications from secondary bacterial infection are a leading cause of morbidity and mortality associated with influenza virus infection (*5*–*8*). Influenza virus can suppress the immune response to a bacterial infection, which can lead to increased bacterial load and decreased survival. This has been shown in both clinical studies and mouse models for multiple bacterial pathogens, including *Streptococcus pneumoniae*, *Haemophilus influenzae*, *S. pyogenes*, and *Staphylococcus aureus* [reviewed in (*5*–*8*)]. Bacterial overgrowth in these models complicates the analysis of other possible causes of morbidity and mortality. Therefore, we sought an alternative model of coinfection lacking this complication.

Legionella pneumophila has recently been recognized as a clinically relevant complication of influenza virus infection (*9*). When mice were infected with a sublethal dose of influenza virus and then coinfected with a sublethal dose of *L. pneumophila*, 100% of coinfected mice died within 1 week of coinfection, whereas all mice survived single infections (Fig. 1A). An established viral infection was necessary for lethality, because mice infected with influenza at the same time or 3 days after infection with *L. pneumophila* survived coinfection (Fig. 1A). A resolved influenza virus infection no longer affected the ability to survive coinfection with *L. pneumophila*, because mice infected with bacteria 10 or 14 days after viral infection also survived (Fig. 1A). The mice coinfected with *L. pneumophila* 3 days after influenza virus infection also had other signs of morbidity, including decreased body weight and temperature (Fig. 1, B and C).

Importantly, despite the dramatic difference in host survival, there was no significant difference in the viral or bacterial pathogen burden after single infections or coinfections (Fig. 1, D and E). Moreover, there was no detectable systemic dissemination of influenza or *L. pneumophila* after infections (fig. S1). These results indicate that lethal synergy between influenza virus and *L. pneumophila* was not due to impaired resistance to either of these pathogens. This is in contrast to coinfections with influenza virus and opportunistic bacterial pathogens where bacterial overgrowth and systemic dissemination are commonly observed (*5*–*8*, *10*–*13*).

[1]Howard Hughes Medical Institute and Department of Immunobiology, Yale University School of Medicine, New Haven, CT 06520, USA. [2]Max F. Perutz Laboratories, University of Vienna, Dr. Bohr Gasse 9/4 A-1030 Vienna, Austria. [3]Department of Pathology, Yale University School of Medicine, New Haven, CT 06520, USA. [4]VA Connecticut Healthcare System Pathology and Laboratory Medicine Service, 950 Campbell Avenue, West Haven, CT 06516, USA.

*Corresponding author. E-mail: ruslan.medzhitov@yale.edu (R.M.); amanda_jamieson@brown.edu (A.M.J.)
†Present address: Department of Molecular Microbiology and Immunology, Brown University, 171 Meeting Street, Providence, RI 02912, USA.
‡These authors contributed equally to this work.

Fig. 1. Decreased tolerance with unchanged resistance of mice coinfected with influenza virus and *L. pneumophila*. (**A**) Survival of mice infected intranasally with 300 plaque-forming units (PFUs) of influenza virus and 0, 3, 6, 10, or 14 days (d) later with 1×10^6 *L. pneumophila*. To better mirror a human infection, mice were infected with a strain of *L. pneumophila* lacking the *flaA* gene (JR32ΔflaA), which encodes flagellin. (**B**) Weight of mice infected with influenza virus or *L. pneumophila* alone or coinfected 3 days after influenza virus. (**C**) Body temperature of mice coinfected 3 days after influenza virus compared with the singly infected controls. (**D**) Lung bacterial load in mice coinfected 3 days after influenza virus or mice infected with *L. pneumophila* alone. Day 0 indicates colony-forming units (CFUs) in the lung 1 hour after infection. (**E**) Lung viral load in mice coinfected 3 days after influenza virus or mice infected in influenza virus alone. (**F**) Survival of mice coinfected 3 days after influenza virus infection with LP01ΔdotA or the thymidine auxotroph LP02 strains of *L. pneumophila*. (**G**) Survival of mice coinfected 3 days after infection with inactivated (IA) influenza virus. Data are combined from at least three independent experiments with at least five mice in each group (*$P \leq 0.05$; **$P \leq 0.001$). Data were analyzed with the logrank test, generalized linear model, or analysis of variance (ANOVA). Error bars represent SD from the mean.

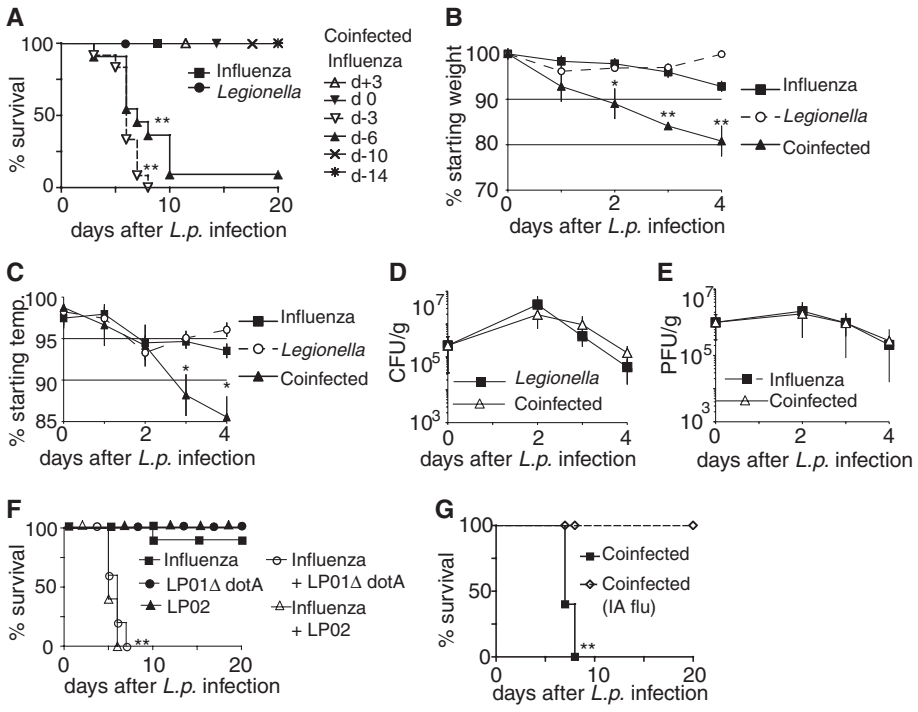

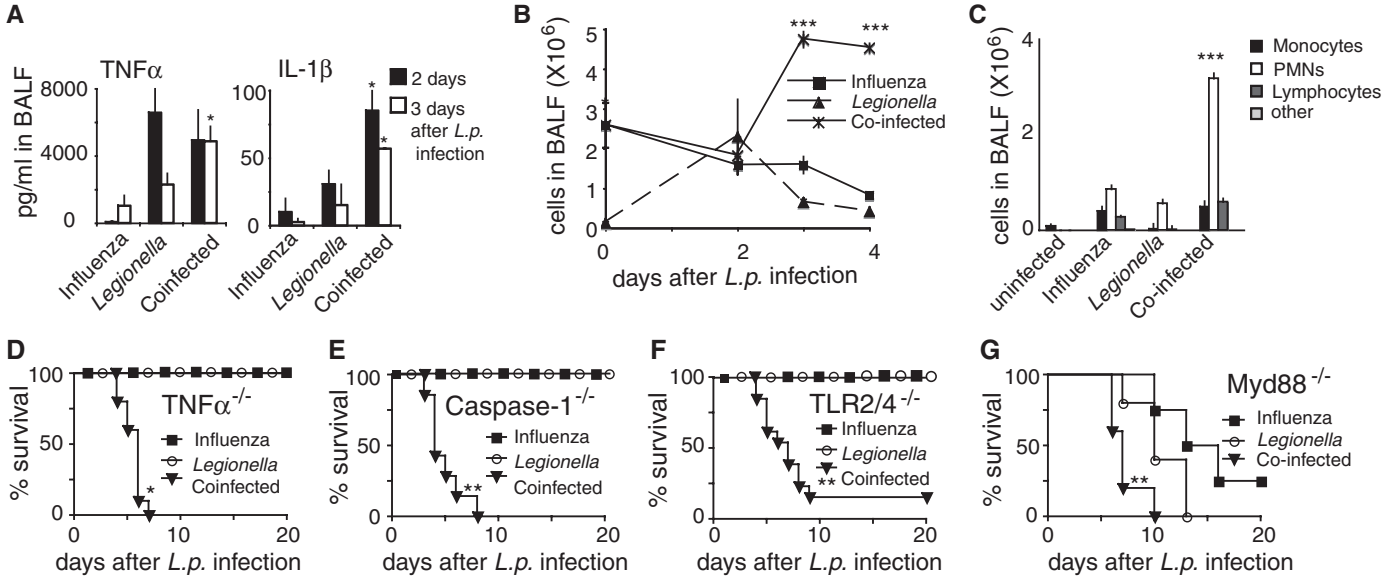

Fig. 2. Decreasing inflammatory pathways does not increase survival of coinfected mice. (**A**) TNF-α and IL-1β levels in the BALF of mice infected with JR32ΔflaA 3 days after influenza virus infection. (**B**) Immune cell infiltrate in BALF of mice coinfected 3 days after influenza virus infection. (**C**) Types of infiltrating cells in the BALF. Survival of (**D**) *Tnf*$^{-/-}$, (**E**) *Casp1*$^{-/-}$, (**F**) *Tlr2*$^{-/-}$*Tlr4*$^{-/-}$, (**G**) *Myd88*$^{-/-}$, (**H**) *Nos2*$^{-/-}$, (**I**) Gr-1–depleted, and (**J**) NK1.1–depleted mice coinfected 3 days after infection with influenza virus compared with singly infected controls (Ctrl.). Data are combined from at least three independent experiments with at least five mice in each group (*$P \leq 0.05$; **$P \leq 0.001$; ***$P \leq 0.0001$). Data were analyzed with the logrank test, *t* test, or ANOVA. Error bars represent SD from the mean.

To further address the role of pathogen virulence, we used an attenuated mutant strain of *L. pneumophila*, which lacks the Dot/Icm type IV secretion system and is therefore unable to secrete virulence factors (*14*). Administration of *dotA* mutant or thymidine auxotroph (LP02) *L. pneumophila*, which are severely attenuated in vivo, still resulted in 100% mortality of coinfected mice (Fig. 1F and fig. S2) (*14*). These results indicate that bacterial virulence or growth is not essential for lethal synergy of influenza–*L. pneumophila* coinfection. Furthermore, mortality is unlikely to be due to failed immune resistance. However, administration of formalin-inactivated influenza virus did not synergize with the subsequent *L. pneumophila* coinfection (Fig. 1G), indicating that a productive virus infection is necessary to make the host sensitive to secondary bacterial infection. Moreover, treatment of mice with neuraminidase inhibitors (NAIs) increased survival and decreased weight loss and hypothermia after coinfection (fig. S3, A to C), presumably because NAIs suppressed viral load (fig. S3D) (*15*).

We next examined whether mortality of influenza–*L. pneumophila* coinfection was due to excessive inflammatory response. Influenza virus activates three innate immune signaling pathways: the (i) Toll-like receptor–MyD88, (ii) RIG-I–interferon-α/β, and (iii) Nlrp3–caspase-1–interleukin-1 pathways (TLR, Toll-like receptor; IFN, interferon; IL, interleukin) (*16*, *17*). *L. pneumophila* is recognized by the innate immune system via several mechanisms, including the Naip5/Birc1e-dependent pathway, which requires an intact Dot/Icm secretion system, and TLRs (*18*–*22*). Gene expression analysis of the lungs after single infection and coinfection indicated that some of the inflammatory genes, including tumor necrosis factor–α (TNF-α), nitric oxide synthase 2 (Nos2), and several chemokines, were expressed at higher levels in coinfected compared with single-infected mice (fig. S4). TNF-α and IL-1β protein levels were also elevated in the broncho-aveolar lavage fluid (BALF) at day 3 after coinfection (Fig. 2A). Moreover, there was a significant increase in neutrophil infiltration in the lungs of coinfected mice compared with singly infected controls (Fig. 2, B and C). TNF-α, IL-1β, Nos2, and neutrophils are all known to play important roles in immunopathology, including in the context of influenza virus infection (*23*–*25*). However, we found that genetic deletions of TNF-α, caspase-1, MyD88, TLR2/4, and Nos2 or antibody-mediated depletion of neutrophils or natural killer cells did not rescue coinfected mice from mortality (Fig. 2, D to J). Similarly, *Rag2*$^{-/-}$ mice, which lack an adaptive immune system, also succumbed to lethal coinfection, indicating that lymphocyte-mediated immunopathology is not essential for the lethal outcome of coinfection (fig. S5A). Virus-induced IFN-α/β can interfere with antibacterial responses (*26*). However, IFN-α/β receptor (IFNAR)–deficient mice (*Ifnar1*$^{-/-}$) were still susceptible to coinfection (fig. S5B). Rag2 and IFNAR knockout mice were also susceptible to influenza infection alone, *Nos2*$^{-/-}$ mice were susceptible to infection with *L. pneumophila* alone, and *Myd88*$^{-/-}$ mice were susceptible to both single infections. However, in all cases, the mortality from coinfections was kinetically distinguishable from that from single infections and was similar to the mortality kinetics of wild-type (WT) mice (Figs. 1A and 2, D to J, and fig. S5, A and B). Finally, systemic treatment of the mice with synthetic glucocorticoid dexamethasone or antioxidant *N*-acetyl cysteine did not rescue them from mortality of coinfection (fig. S5, C and D). Collectively, the elimination of all major immune and inflammatory pathways triggered by either the viral or bacterial infection did not rescue the lethal synergy. These results suggest that the lethal outcome of coinfection in our model was not solely due to excessive inflammatory response or immunopathology.

Because neither bacterial growth or virulence nor host immune responses were individually required to cause lethality in coinfection, we next combined host immunodeficiency and bacterial attenuation. We used a severely attenuated *L. pneumophila* strain LP02ΔdotAΔflaA, which lacks flaA and dotA and is also a thymidine auxotroph (*27*). This strain lacks flagellin and is unable to replicate and secrete effectors, thus lacking major immunostimulatory factors, except

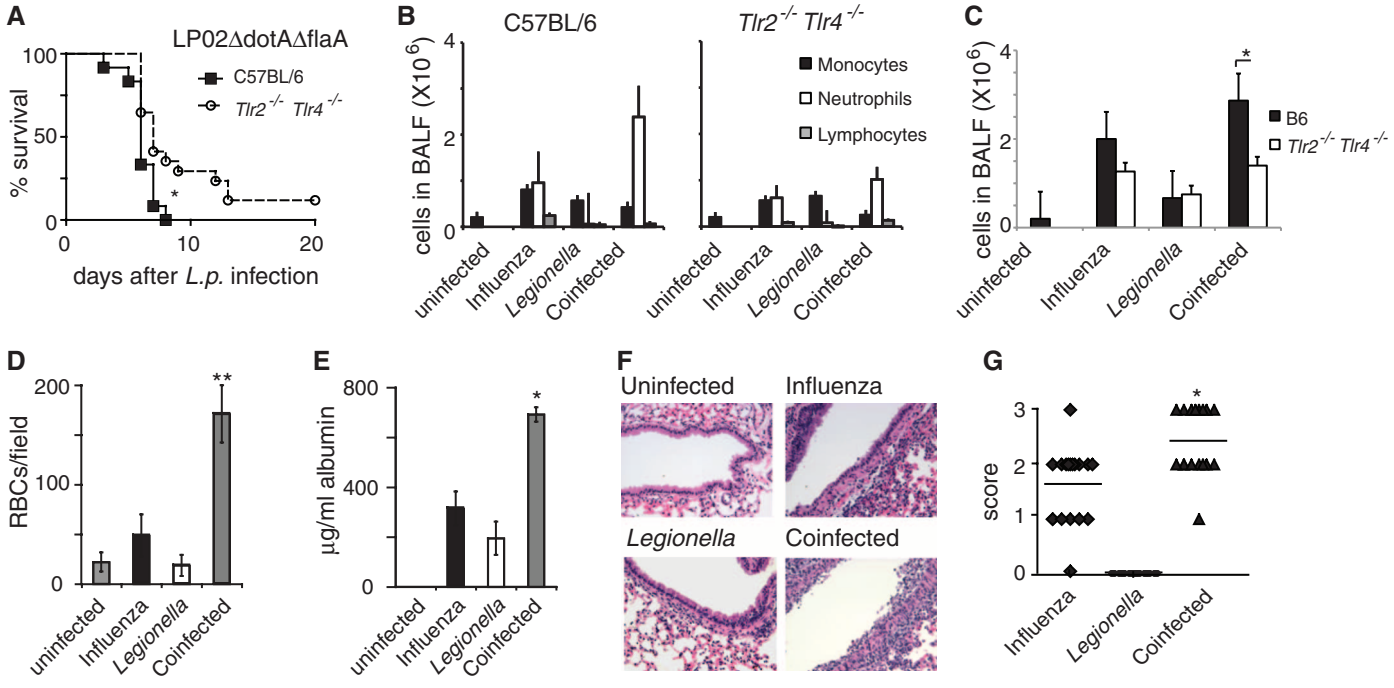

Fig. 3. Increased tissue damage in coinfected lungs. (**A**) Survival of *Tlr2*$^{-/-}$/*Tlr4*$^{-/-}$ and C57BL/6 mice coinfected with the LP02ΔdotAΔflaA strain of *L. pneumophila*. (**B**) Types of infiltrating cells in BALF of *Tlr2*$^{-/-}$/*Tlr4*$^{-/-}$ and C57BL/6 mice coinfected with strain LP02ΔdotAΔflaA 3 days after influenza virus infection. (**C**) Amount of infiltrating immune cells in BALF of *Tlr2*$^{-/-}$/*Tlr4*$^{-/-}$ and C57BL/6 mice coinfected with strain LP02ΔdotAΔflaA 3 days after influenza virus infection. (**D**) Red blood cells (RBCs) and (**E**) albumin in the BALF day 4 after bacterial infection in C57BL/6 mice infected with influenza virus and 3 days later with the JR32ΔflaA strain. (**F**) Representative images of airways and (**G**) histological damage scoring of lung sections 4 days after bacterial infection from C57BL/6 mice infected with influenza virus and 3 days later with the JR32ΔflaA strain. Data are combined from at least three independent experiments with at least five mice in each group (*$P \leq 0.05$; **$P \leq 0.001$). Data were analyzed using the logrank test, *t* test, or ANOVA. Error bars represent SD from the mean.

for cell-wall components detectable by TLR2 and TLR4. Therefore, we used this strain to coinfect TLR2/TLR4 double-deficient mice. *Tlr2*$^{-/-}$/*Tlr4*$^{-/-}$ mice coinfected with influenza virus and LP02ΔdotAΔflaA had a small increase in survival compared with WT mice infected with the same strain of bacteria (Fig. 3A); however, most mice still succumbed to coinfection. *Tlr2*$^{-/-}$/*Tlr4*$^{-/-}$ mice coinfected with LP02ΔdotAΔflaA had decreased immune cell infiltrate into the BALF at day 3 after infection, when compared with C57BL/6 mice infected with either LP02ΔdotAΔflaA or Jr32ΔflaA (Figs. 2, B and C, and 3, B and C). Thus, severely attenuated, nonreplicating *L. pneumophila* still caused mortality in coinfected *Tlr2*$^{-/-}$/*Tlr4*$^{-/-}$ mice, despite almost a complete lack of immunostimulatory signals.

The lethal outcome of influenza–*L. pneumophila* coinfection, despite normal control of pathogen growth, suggests that the mortality could be due to a failed tolerance to tissue damage caused by coinfection. Coinfected mice had high levels of red blood cells and albumin in the BALF (Fig. 3, D and E), indicating a damage to the lung epithelial-capillary barrier (*28*). The lung epithelial damage was further confirmed by histological analysis (Fig. 3, F and G). The principal difference among the singly infected and coinfected mice was in the degree of airway epithelial necrosis, with the coinfected lungs having a significant increase in epithelial cell damage. Extensive damage to the airway epithelia, with secondary alveolar collapse (Fig. 3, D to G), is presumably responsible for the mortality of the coinfection.

Consistent with the histological evidence of lung tissue damage, a gene expression analysis revealed that a cohort of genes involved in tissue protection and repair was specifically downregulated in coinfected compared with singly infected or uninfected mice. This cohort included genes that are essential for tissue and cellular repair and development in the lung, such as *Mdk*, *Adamts2*, *Timp4*, *Slpi*, *Mmp2*, *Mmp9*, *Vegfc*, *Itgb7*, and *Itga1* (*29*), as well as genes involved in stress response in lung tissue, such as *Gcnt2*, *Hif3a*, *Stra13*, *Hmox1*, and *Aifm1* (*30*) (fig. S6).

We next tested whether the defective expression of the tissue-repair program is responsible for mortality of coinfection. Amphiregulin (AREG), an epithelial growth factor family member, was recently found to contribute to tissue homeostasis in the lung during influenza infection (*31*). Although AREG did not have a significant effect in WT mice, administration of AREG to *Tlr2*$^{-/-}$/*Tlr4*$^{-/-}$ mice coinfected with influenza virus and the LP02ΔdotAΔflaA strain of *L. pneumophila* significantly increased survival while decreasing weight loss and hypothermia (Fig. 4, A to C). AREG treatment resulted in decreased lung damage, as indicated by histopathological analysis, decreased albumin level in the BALF, and decreased pulmonary infiltrate (Fig. 4, D to G). Importantly, AREG treatment significantly decreased mortality of coinfection (Fig. 4A) but did not affect the viral and bacterial burdens (Fig. 4, H and I). The reason AREG administration did not rescue WT mice from coinfection is likely because, in this case, the disease is too severe and may require a more optimal regimen of AREG administration or, perhaps, additional methods of promoting tissue protection and repair.

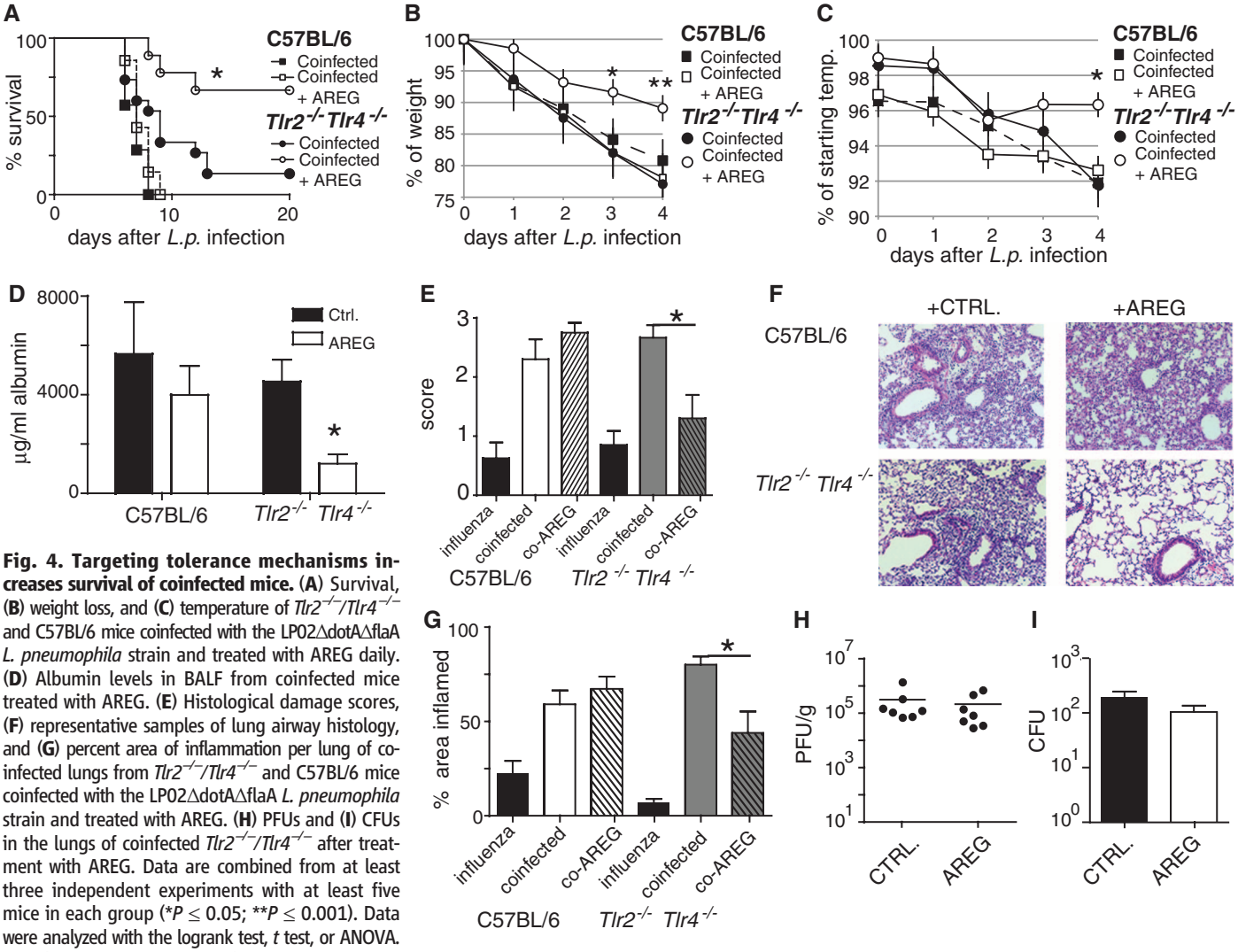

Fig. 4. Targeting tolerance mechanisms increases survival of coinfected mice. (**A**) Survival, (**B**) weight loss, and (**C**) temperature of *Tlr2*$^{-/-}$/*Tlr4*$^{-/-}$ and C57BL/6 mice coinfected with the LP02ΔdotAΔflaA *L. pneumophila* strain and treated with AREG daily. (**D**) Albumin levels in BALF from coinfected mice treated with AREG. (**E**) Histological damage scores, (**F**) representative samples of lung airway histology, and (**G**) percent area of inflammation per lung of coinfected lungs from *Tlr2*$^{-/-}$/*Tlr4*$^{-/-}$ and C57BL/6 mice coinfected with the LP02ΔdotAΔflaA *L. pneumophila* strain and treated with AREG. (**H**) PFUs and (**I**) CFUs in the lungs of coinfected *Tlr2*$^{-/-}$/*Tlr4*$^{-/-}$ after treatment with AREG. Data are combined from at least three independent experiments with at least five mice in each group (*$P \leq 0.05$; **$P \leq 0.001$). Data were analyzed with the logrank test, *t* test, or ANOVA. Error bars represent SD from the mean.

Collectively, these results demonstrate that (i) lethal synergy of influenza virus and bacterial coinfection can result from loss of tolerance to infection-induced tissue damage, (ii) morbidity and mortality of coinfection can be independent of pathogen burden or excessive inflammatory response, and (iii) promoting tissue repair can, in principle, rescue coinfected animals from morbidity and mortality, even without affecting pathogen burden. Finally, our influenza–*L. pneumophila* coinfection model demonstrates the distinction between resistance and tolerance as separate host defense strategies that can both contribute to morbidity and mortality of infectious disease.

References and Notes

1. L. Råberg, D. Sim, A. F. Read, *Science* **318**, 812 (2007).
2. L. Råberg, A. L. Graham, A. F. Read, *Philos. Trans. R. Soc. London Ser. B Biol. Sci.* **364**, 37 (2009).
3. D. S. Schneider, J. S. Ayres, *Nat. Rev. Immunol.* **8**, 889 (2008).
4. R. Medzhitov, D. S. Schneider, M. P. Soares, *Science* **335**, 936 (2012).
5. C. Beadling, M. K. Slifka, *Curr. Opin. Infect. Dis.* **17**, 185 (2004).
6. J. A. McCullers, *Clin. Microbiol. Rev.* **19**, 571 (2006).
7. J. M. Hament, J. L. Kimpen, A. Fleer, T. F. Wolfs, *FEMS Immunol. Med. Microbiol.* **26**, 189 (1999).
8. V. T. Peltola, J. A. McCullers, *Pediatr. Infect. Dis. J.* **23** (suppl.), S87 (2004).
9. M. Iannuzzi *et al.*, *J. Med. Case Rep.* **5**, 520 (2011).
10. A. Shahangian *et al.*, *J. Clin. Invest.* **119**, 1910 (2009).
11. A. R. Iverson *et al.*, *J. Infect. Dis.* **203**, 880 (2011).
12. K. Sun, D. W. Metzger, *Nat. Med.* **14**, 558 (2008).
13. A. Didierlaurent *et al.*, *J. Exp. Med.* **205**, 323 (2008).
14. K. H. Berger, R. R. Isberg, *Mol. Microbiol.* **7**, 7 (1993).
15. D. B. Mendel *et al.*, *Antimicrob. Agents Chemother.* **42**, 640 (1998).
16. T. Ichinohe, *Expert Rev. Vaccines* **9**, 1315 (2010).
17. A. García-Sastre, C. A. Biron, *Science* **312**, 879 (2006).
18. T. Ren, D. S. Zamboni, C. R. Roy, W. F. Dietrich, R. E. Vance, *PLoS Pathog.* **2**, e18 (2006).
19. A. B. Molofsky *et al.*, *J. Exp. Med.* **203**, 1093 (2006).
20. D. S. Zamboni *et al.*, *Nat. Immunol.* **7**, 318 (2006).
21. K. A. Archer, C. R. Roy, *Infect. Immun.* **74**, 3325 (2006).
22. R. Spörri, N. Joller, U. Albers, H. Hilbi, A. Oxenius, *J. Immunol.* **176**, 6162 (2006).
23. N. L. La Gruta, K. Kedzierska, J. Stambas, P. C. Doherty, *Immunol. Cell Biol.* **85**, 85 (2007).
24. J. S. M. Peiris, K. P. Y. Hui, H.-L. Yen, *Curr. Opin. Immunol.* **22**, 475 (2010).
25. N. Schmitz, M. Kurrer, M. F. Bachmann, M. Kopf, *J. Virol.* **79**, 6441 (2005).
26. T. Decker, M. Müller, S. Stockinger, *Nat. Rev. Immunol.* **5**, 675 (2005).
27. M. F. Fontana, S. Shin, R. E. Vance, *Infect. Immun.* **80**, 3570 (2012).
28. D. K. Bhalla, *J. Toxicol. Environ. Health B Crit. Rev.* **2**, 31 (1999).
29. L. M. Crosby, C. M. Waters, *Am. J. Physiol. Lung Cell. Mol. Physiol.* **298**, L715 (2010).
30. H. R. Wong, J. R. Wispé, *Am. J. Physiol.* **273**, L1 (1997).
31. L. A. Monticelli *et al.*, *Nat. Immunol.* **12**, 1045 (2011).

Acknowledgments: We thank S. Holley and C. Annicelli for technical assistance; T. Ichinohe, M. Linehan, and A. Iwasaki for viral strains and advice; T. Ren, M. Fontana, R. Vance, K. Archer, S. Shin, and C. Roy for *L. pneumophila* strains and advice; M. Gillum for assistance with experiments; and M. Mueller and C. Lassnig for mouse infection infrastructure. The data presented in the manuscript are tabulated in the main paper and in the supplementary materials. This work was supported by the Howard Hughes Medical Institute (R.M.), NIH grants R01 046688 and AI R01 055502 (R.M.), the Ellison Foundation (R.M.), the New England Regional Center of Excellence (R.M.), and FWF (Austrian Science Fund) grant P25235-B13 (A.M.J.). A.M.J. was a Berger Foundation fellow of the Damon Runyon Cancer Research Foundation. The authors have no conflicts of interest.

Supplementary Materials

www.sciencemag.org/cgi/content/full/science.1233632/DC1
Supplementary Text
Figs. S1 to S6
References (*32*, *33*)

4 December 2012; accepted 15 April 2013
Published online 25 April 2013;
10.1126/science.1233632

Repeated Cortico-Striatal Stimulation Generates Persistent OCD-Like Behavior

Susanne E. Ahmari,[1,2,3,4]* Timothy Spellman,[5] Neria L. Douglass,[1,2] Mazen A. Kheirbek,[1,2] H. Blair Simpson,[1,3,4] Karl Deisseroth,[6] Joshua A. Gordon,[1,2] René Hen[1,2]

Although cortico-striato-thalamo-cortical (CSTC) circuit dysregulation is correlated with obsessive compulsive disorder (OCD), causation cannot be tested in humans. We used optogenetics in mice to simulate CSTC hyperactivation observed in OCD patients. Whereas acute orbitofrontal cortex (OFC)–ventromedial striatum (VMS) stimulation did not produce repetitive behaviors, repeated hyperactivation over multiple days generated a progressive increase in grooming, a mouse behavior related to OCD. Increased grooming persisted for 2 weeks after stimulation cessation. The grooming increase was temporally coupled with a progressive increase in light-evoked firing of postsynaptic VMS cells. Both increased grooming and evoked firing were reversed by chronic fluoxetine, a first-line OCD treatment. Brief but repeated episodes of abnormal circuit activity may thus set the stage for the development of persistent psychopathology.

OCD is characterized by intrusive distressing thoughts (obsessions) and/or repetitive mental or behavioral acts (compulsions) and is a leading cause of illness-related disability (*1*, *2*). Although the pathophysiology underlying OCD is unclear, multiple lines of evidence implicate dysregulation within cortico-striato-thalamo-cortical (CSTC) circuits (*3*–*6*). Specifically, functional imaging studies suggest that hyperactivity in orbitofrontal cortex (OFC) and ventromedial striatum (VMS) is associated with OCD pathology (*5*, *7*, *8*). Furthermore, successful treatments are associated with reductions in hyperactivity (*9*, *10*). However, it is not known if OFC-VMS hyperactivity can directly cause OCD symptoms, because increased activity could represent adaptive, homeostatic, or unrelated processes compensating for other primary abnormalities. We therefore used an optogenetic strategy to directly test whether hyperstimulation of glutamatergic OFC-VMS projections leads to OCD-like behaviors in mice.

A Cre-inducible adenovirus-associated vector (AAV) carrying the gene encoding channelrhodopsin (ChR2) fused to enhanced yellow fluorescent protein (EYFP) [pAAV-Ef1a-DIO-ChR2 (H134R)-EYFP; referred to as DIO-ChR2] (*11*) was stereotactically injected into OFC of EMX-Cre transgenic mice to ensure specific ChR2 expression in cortical glutamatergic neurons (Fig. 1A) (*12*). Cortical Cre expression led to sustained expression of ChR2-EYFP (Fig. 1B). Unilateral 473-nm stimulation through chronic fiber-optic implants in OFC yielded lateralized increased activation of the immediate early gene c-*fos* ($P < 0.009$) (Fig. 1, C and D), which demonstrated in vivo cellular activation by laser stimulation. Two weeks postinjection, EYFP staining was seen in OFC cell bodies and axons projecting to VMS (Fig. 1E), which indicated targeting of OFC-VMS projections. In vitro recordings in cortico-striatal slices demonstrated VMS field responses after 473-nm laser stimulation of OFC axon terminals in striatum (Fig. 1F). To verify adequate stimulation of ChR2-expressing OFC-VMS terminals in vivo, we implanted stereo opto-electrodes (optrodes) into VMS that permit combined fiber-optic stimulation and 32-channel simultaneous recording of multiple single units (Fig. 1G). In awake behaving mice, in vivo recordings demonstrated robust VMS field responses after 473-nm laser stimulation of OFC axon terminals in striatum (Fig. 1, H and I), which showed

[1]Department of Psychiatry, Columbia University College of Physicians and Surgeons, New York, NY 10032, USA. [2]Division of Integrative Neuroscience, New York State Psychiatric Institute, New York, NY 10032, USA. [3]Division of Clinical Therapeutics, New York State Psychiatric Institute, New York, NY 10032, USA. [4]Anxiety Disorders Clinic and OCD Research Program, New York State Psychiatric Institute, New York, NY 10032, USA. [5]Department of Physiology, Columbia University College of Physicians and Surgeons, New York, NY 10032, USA. [6]Departments of Psychiatry and Bioengineering, Stanford University School of Medicine, Stanford, CA 94305, USA.

*Corresponding author. E-mail: sea2103@columbia.edu

Role of Tissue Protection in Lethal Respiratory Viral-Bacterial Coinfection

Amanda M. Jamieson, Lesley Pasman, Shuang Yu, Pia Gamradt, Robert J. Homer, Thomas Decker, and Ruslan Medzhitov

Science, **340** (6137), .
DOI: 10.1126/science.1233632

Tolerance Needed

It's a common enough occurrence: You're sick as a dog with a cold, but the person in the office next door just has a few sniffles. What accounts for this difference? Most commonly, these sorts of differences are chalked up to differences in resistance—perhaps you have higher viral loads than your office mate. But such differences can also involve differences in the ability to tolerate the same amount of virus. Deciphering the contribution of resistance versus tolerance, however, is difficult. Jamieson *et al.* (p. 1230, published online 25 April) studied a mouse model of viral and bacterial co-infection where tolerance and resistance could be separated. Mice infected with influenza virus were more likely to succumb to a secondary infection with *Legionella pneumophila* as a result of impaired tolerance to tissue damage, rather than because of a difference in bacterial burden.